PNAS RESEARCH ARTICLE | DEVELOPMENTAL BIOLOGY

Wdr59 promotes or inhibits TORC1 activity depending on cellular context

Yingbiao Zhang[a], Chun-Yuan Ting[a], Shu Yang[a], John Reich[a], Karenne Fru[a], and Mary A. Lilly[a,1]

Edited by Michael Hall, Universitat Basel, Basel, Switzerland; received July 18, 2022; accepted October 23, 2022

Target of Rapamycin Complex I (TORC1) is a central regulator of metabolism in eukaryotes that responds to a wide array of negative and positive inputs. The GTPase-activating protein toward Rags (GATOR) signaling pathway acts upstream of TORC1 and is comprised of two subcomplexes. The trimeric GATOR1 complex inhibits TORC1 activity in response to amino acid limitation by serving as a GTPase-activating protein (GAP) for the TORC1 activator RagA/B, a component of the lysosomally located Rag GTPase. The multi-protein GATOR2 complex inhibits the activity of GATOR1 and thus promotes TORC1 activation. Here we report that Wdr59, originally assigned to the GATOR2 complex based on studies performed in tissue culture cells, unexpectedly has a dual function in TORC1 regulation in *Drosophila*. We find that in the ovary and the eye imaginal disc brain complex, Wdr59 inhibits TORC1 activity by opposing the GATOR2-dependent inhibition of GATOR1. Conversely, in the *Drosophila* fat body, Wdr59 promotes the accumulation of the GATOR2 component Mio and is required for TORC1 activation. Similarly, in mammalian HeLa cells, Wdr59 prevents the proteolytic destruction of GATOR2 proteins Mio and Wdr24. Consistent with the reduced levels of the TORC1-activating GATOR2 complex, Wdr59KOs HeLa cells have reduced TORC1 activity which is restored along with GATOR2 protein levels upon proteasome inhibition. Taken together, our data support the model that the Wdr59 component of the GATOR2 complex functions to promote or inhibit TORC1 activity depending on cellular context.

Wdr59 | TORC1 | GATOR1 | GATOR2 | *Drosophila*

Significance

TORC1 promotes anabolic metabolism and growth and is frequently deregulated in human diseases, including epilepsy and cancer. The GATOR complex acts upstream of TORC1 to regulate the response to nutrient limitation and is required for the maintenance of metabolic homeostasis. Here we use whole animal studies in *Drosophila*, coupled with work in mammalian HeLa cells, to define two functions of the GATOR component Wdr59. Surprisingly, we find that the role of Wdr59 in TORC1 regulation is tissue specific, with Wdr59 functioning to promote or inhibit TORC1 activity depending on cellular context. These studies broaden our understanding of the GATOR-TORC1 signaling axis in metazoans and highlight the complexity of metabolic regulation in vivo.

The highly conserved Target of Rapamycin Complex 1 (TORC1) is a central regulator of growth and metabolism in eukaryotes (1–4). In the presence of positive upstream inputs, TORC1 promotes anabolic metabolism and growth by phosphorylating numerous downstream targets including S6K and 4EBP. Conversely, when exposed to negative cues, such as limited nutrients, or the lack of growth factors, cells downregulate TORC1 to activate catabolic metabolism and inhibit growth. The deregulation of TORC1 is implicated in a wide array of diseases including cancer, epilepsy, and aging (1, 5). Thus, there is intense interest in obtaining a mechanistic understanding of how upstream signaling pathways regulate TORC1 activity.

The Rag GTPase is a heterodimer comprised of a Rag A/B subunit and a RagC/D subunit, that recruits TORC1 to lysosomes for activation by the small GTPase Rheb, when the RagA/B component of the GTPase is in the GTP-bound state (6–8). The GTPase-activating protein toward Rags (GATOR) complex is an important upstream regulator of TORC1 that responds to the presence of nutrients (1, 9). The GATOR complex, originally identified in yeast and named the Seh1 Associated (SEA) complex, is comprised of two subcomplexes, GATOR1 and GATOR2 (Fig. 1*A*) (9–12). The GATOR1 complex, which contains the proteins Nprl2, Nprl3, and DEPDC5/Iml1, inhibits TORC1 activity by serving as a GAP (GTPase-activating protein) for the lysosomally located Rag GTPase (9, 12).

The GATOR2 complex inhibits GATOR1 and thus serves to activate TORC1 (9, 12, 13). However, the mechanism by which GATOR2 inhibits GATOR1 remains unknown. In its initial functional characterization in mammalian and *Drosophila* cultured cells, the GATOR2 complex was reported to contain five protein Mios/Mio, Seh1, Sec13, Wdr24, and Wdr59 (Fig. 1*A*) (9). In these studies, knockdowns of GATOR2 components resulted in the constitutive activation of GATOR1 and decreased TORC1 activity. Similarly, *Drosophila* mutants of the GATOR2 components *mio*, *seh1*, and *wdr24* exhibit decreased TORC1 activity and growth in the female germline (13–16). However, a recent study from *Schizosaccharomyces pombe* reported that SEA3/WDR59 inhibits TORC1 activity as a component of the GATOR1 complex (17). Notably, this is oppositive to the role assigned to Wdr59 based on studies in both human and *Drosophila* cultured cells (9, 18, 19). Additionally, deletions of Wdr59 in HEK293 cells and mouse embryonic

Author contributions: Y.Z., C.-Y.T., S.Y., J.R., K.F., and M.A.L. designed research; Y.Z., C.-Y.T., S.Y., J.R., and K.F. performed research; Y.Z., C.-Y.T., S.Y., K.F., and M.A.L. analyzed data; and Y.Z. and M.A.L. wrote the paper.

The authors declare no competing interest.

This article is a PNAS Direct Submission.

[1]To whom correspondence may be addressed. Email: lillym@nih.gov.

This article contains supporting information online at https://www.pnas.org/lookup/suppl/doi:10.1073/pnas.2212330120/-/DCSupplemental.

Published December 28, 2022.

fibroblasts result in a partial resistance to nutrient deprivation (20). Thus, the exact function of Wdr59 within the GATOR-TORC1 signaling pathway remains unclear.

Here we define the in vivo requirement for the GATOR component Wdr59 in *Drosophila*. We find that Wdr59 displays two distinct functions depending on cell type. First, in the ovary and the eye imaginal disc brain complex, Wdr59 acts upstream of the GATOR2 complex to inhibit TORC1 activity. Second, in the adult fat body and mammalian HeLa cells, Wdr59 protects the GATOR2 complex from proteolysis and promotes TORC1 activity. Our data provide mechanistic insight into the complex role of the GATOR component Wdr59 in the tissue-specific regulation of TORC1 activity.

Results

Wdr59 Inhibits TORC1 Activity and Cell Growth in the *Drosophila* Ovary. Previous functional studies from cultured cells assigned Wdr59 to the GATOR2 complex, with an essential role in TORC1 activation (9). However, whole animal studies in *Drosophila* revealed that there are tissue-specific requirements for the GATOR2 components Mio, Seh1, and Wdr24 in the regulation of TORC1 activity (13–16). Therefore, to define the in vivo requirement for Wdr59 in *Drosophila*, we generated a *wdr59* null allele, $wdr59^{1}$, that deleted 90% of the *wdr59* open reading frame (*SI Appendix,* Fig. S1). As is observed with null mutants of other GATOR2 components, including mio^{ko2}, $seh1^{D15}$, and $wdr24^{1}$, $wdr59^{1}$ mutants are viable. However, while *mio*, *seh1*, and *wdr24* mutants have small ovaries and are female sterile, $wdr59^{1}$ mutants are fertile with ovaries significantly larger than ovaries from wild-type (WT) females (Fig. 1 *B* and *C*) (13–16). The increase in ovary size suggested that, in contrast to other components of the GATOR2 complex, Wdr59 may function to restrict ovarian growth. To test this hypothesis, and to determine if *wdr59* acts cell autonomously, we generated $wdr59^{1}$ homozygous germline clones using the Nanos Flippase Recognition Target/ Recombinase Flippase FLP/FRT system (18, 21). The ovaries of *Drosophila* females contain approximately 15 ovarioles each consisting of a string of sequentially developing egg chambers. In WT ovaries, the posterior egg chamber is always older and larger than the adjacent anterior egg chamber. Consistent with the idea that Wdr59 inhibits growth, egg chambers containing homozygous germline clones of $wdr59^{1}$ mutant cells (marked by arrow) were larger than the adjacent posterior egg chambers containing $wdr59^{1}$/+ heterozygous cells (Fig. 1 *D*–*G*). Thus, like components of the GATOR1 complex, *wdr59* acts cell autonomously to inhibit growth in the female germline of *Drosophila* (*SI Appendix,* Fig. S2).

To determine if the increased growth observed in $wdr59^{1}$ ovaries is accompanied by increased TORC1 activity, we compared the

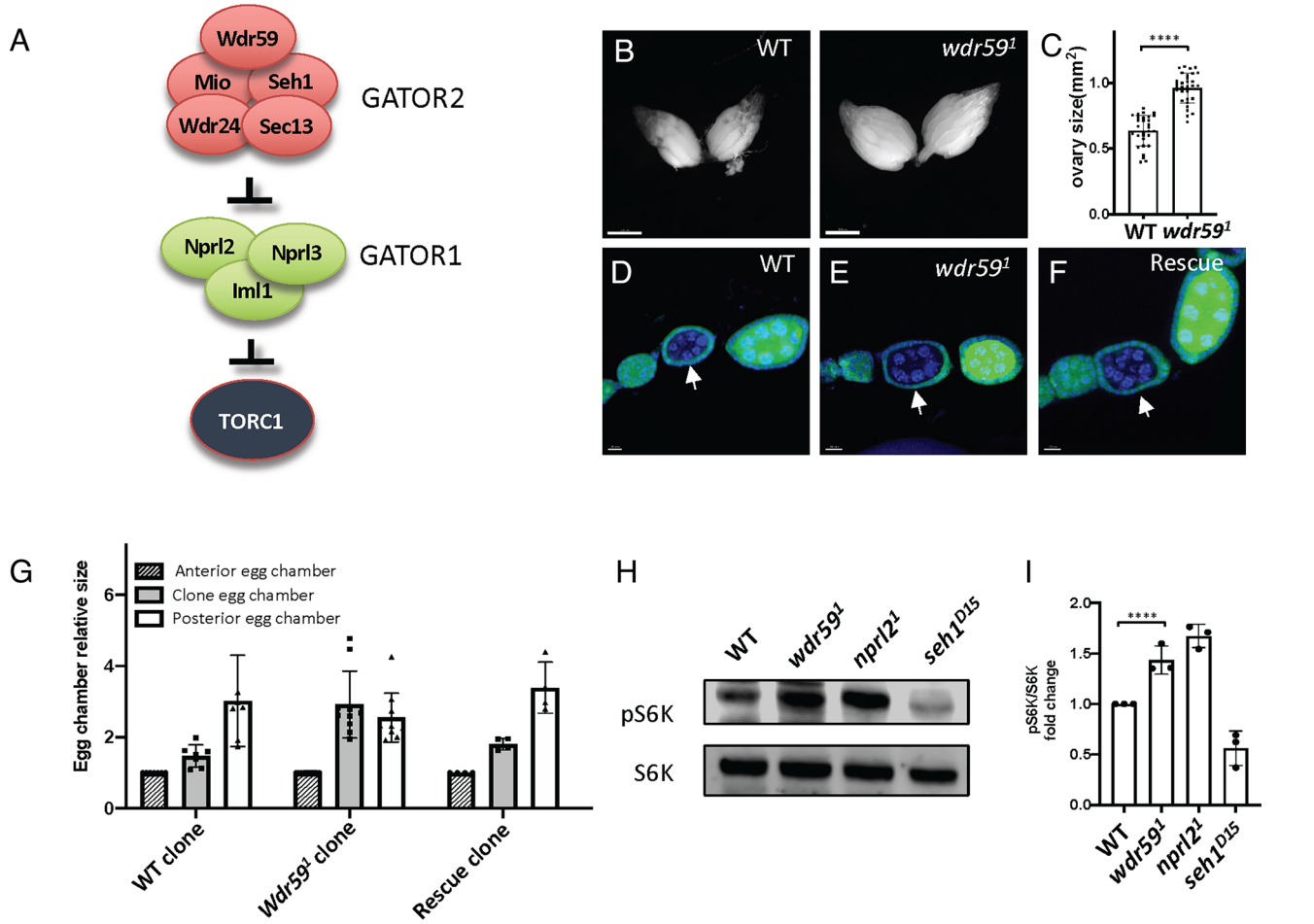

Fig. 1. $wdr59^{1}$ mutant ovaries have increased cell growth and TORC1 activity. (*A*) The GATOR complex regulates TORC1 activity. (*B*) Ovaries from Canton-S (WT) and $wdr59^{1}$ mutant females. (*C*) Quantification of ovary size (μm^2) from (*B*). (*D*) WT and (*E*) $wdr59^{1}$ germline clones marked by the absence of Green Fluorescent Protein (GFP) and co-stained with Hoechst to mark DNA. (*F*) $wdr59^{1}$ mutant increased germline clone size is rescued by the wdr59 BAC (2L:11,054,726- 11,151,517) site-specific insertion. (*G*) Quantification of relative size of egg chambers containing WT and $wdr59^{1}$ mutant germline clones relative to adjacent heterozygous egg chambers. The egg chambers anterior (younger) to the egg chamber containing the germline clone were used for normalization. (*H*) Western blot of p-S6K and total-S6K levels of whole ovaries prepared from WT, $wdr59^{1}$, $nprl2^{1}$ and $seh1^{D15}$ *mutant* females. (*I*) Quantification of p-S6K levels relative to total S6K by Western blot from (*H*) (N = 3). (Scale bar, 500 μm.) (*B*), 10 μm (*D*–*F*). Unpaired Student's *t* test was used to calculate statistical significance. Error bars represent SD. ****$P < 0.0001$.

phosphorylation status of S6 kinase, a downstream TORC1 target (22) in WT versus *wdr59*^{1} mutant ovaries. Consistent with our examination of ovarian growth, we found that, *wdr59*^{1} mutant ovaries had increased in TORC1 activity relative to ovaries from WT females. Indeed, *wdr59*^{1} ovaries had levels of pS6K that were only slightly below the levels observed in mutant ovaries from the GATOR1 component *nprl2*^{1}(Fig. 1 *H* and *I*). Additionally, over-expression of Wdr59 using the germline-specific drive nos-GAL4 lowered TORC1 activity in the ovary (*SI Appendix,* Fig. S3). Taken together, our data demonstrate that Wdr59 inhibits both TORC1 activity and growth in the female germline. Notably, these phenotypes are more consistent with the function of the TORC1 inhibitory complex GATOR1 than the TORC1 activator GATOR2.

Wdr59 Promotes the Response to Nutrient Stress. *Drosophila* oogenesis is highly sensitive to nutritional inputs (23–26). In response to conditions of nutrient limitation, the growth rate in young egg chambers (stages 2 to 7) is sharply limited in a process that requires the GATOR1 complex (14, 27). Therefore, we next examined if like the GATOR1 complex, Wdr59 is required for the response to nutrient stress. Toward this end, we starved females that contained either WT or *wdr59*^{1} germline clones on PBS for 12 h and then compared growth patterns in the two clonal genotypes (Fig. 2 *A* and *B*). Notably, the difference in growth rates between WT and *wdr59*^{1} clones was greater in starved relative to fed conditions (Fig. 2 *A* and *B*). The increased size difference between WT and *wdr59*^{1} mutant clones under starved conditions could be explained, if adjacent WT egg chambers limited their growth during amino acid starvation, while the *wdr59*^{1} mutant egg chambers did not. In line with this hypothesis, ovaries from starved homozygous *wdr59*^{1} females had increased TORC1 activity relative to WT ovaries (Fig. 2 *C* and *D*). These data are consistent with the model that Wdr59 facilitates the response to nutrient stress by inhibiting TORC1 activity. However, as is observed in mammalian cells, while the response to nutrient stress is blunted, it is not absent (20). *wdr59*^{1} mutant ovaries respond to nutrient stress by lowering TORC1 activity, but not to the level observed in WT females. Therefore, it is currently not clear if Wdr59 is a component of a pathway that actively participates in the response to nutrient stress or if Wdr59 is generally required to restrain TORC1 activity in all nutrient conditions.

High TORC1 activity inhibits catabolic metabolism and autophagy. Thus, we next examined if high TORC1 activity blocked the induction of autophagy in the *wdr59*^{1} female germline during periods of starvation. Egg chambers from starved WT females accumulate numerous Atg8 positive puncta which we have previously demonstrated to be autolysosomes (14, 28) (Fig. 2 *E* and *F*). In contrast, egg chambers from *wdr59*^{1}-starved females fail to accumulate large Atg8 puncta in response to starvation (Fig. 2*F*). These data support the hypothesis that Wdr59 is required to inhibit TORC1 activity, to afford the full activation of the autophagic response in the *Drosophila* ovary.

Wdr59 Restricts TORC1 Activity Upstream of the GATOR2 Complex. In tissue culture cells, Wdr59 promotes TORC1 activity, presumably as a component of the GATOR2 complex (29). However, our data indicate that like components of the GATOR1 complex Wdr59 inhibits TORC1 activity and growth and promotes autophagy in the female germline. In tissue culture cells and the *Drosophila* ovary, the GATOR2 complex inhibits GATOR1, thereby preventing the constitutive downregulation of TORC1 activity (13, 14, 29, 30). Thus, GATOR1 is epistatic to GATOR2, with double mutants of GATOR1 and GATOR2 components having a GATOR1 phenotype (13, 14, 29). To determine if like GATOR1, *wdr59* is epistatic to GATOR2 in the female germline, we examined *wdr59*^{1}, *mio*^{ko2}and *wdr59*^{1}, *seh1*^{D15} double-mutant ovaries. We found that in contrast to what is observed with GATOR1, the *mio*^{ko2} and *seh1*^{D15} small ovary phenotypes were not rescued in the *wdr59*^{1}, *mio*^{ko2} and *wdr59*^{1}, *seh1*^{D15} double mutants (Fig. 3 *A* and *B*) (13, 14, 27). Consistent with this result, TORC1 activity remains low in *wdr59*^{1}, *mio*^{ko2} double-mutant ovaries, similar to what is observed in *mio*^{ko2} single mutants (Fig. 3 *G* and *H*). To demonstrate that this epistatic relationship was due to cell autonomous function in the female germline, we generated *wdr59*^{1}, *mio*^{ko2} (Fig. 3*C*) and *wdr59*^{1}, *wdr24*^{1} (Fig. 3*E*) double-mutant homozygous germline clones. Notably the growth of the double-mutant egg chambers was inhibited as is observed in *mio*^{ko2} and *seh1*^{D15} single mutants (Fig. 3 *C–F* and *SI Appendix*, Fig. S2). Taken together, these data strongly support the model that, unlike the GATOR1 complex components Nprl2, Nprl3, or Iml1, Wdr59 acts upstream of the GATOR2 complex to inhibit TORC1 activity.

Wdr59 Promotes the Association of GATOR1 with the Rag GTPase. How might Wdr59 facilitate the inhibition of TORC1 activity upstream of the GATOR2 complex? The GATOR1 complex acts as a GAP toward RagA, promoting the conversion of RagA^{GTP}, which is competent to recruit TORC1 to lysosomes, to the inactive RagA^{GDP} state (9, 12, 31). Therefore, we examined the association of the GATOR1 component Nprl2 and RagA in *wdr59*^{1} and *wdr24*^{1} mutant ovaries by co-immunoprecipitation(co-IP) using a Nprl2-T7-GFP^{11} knockin and RagA-GFP genomic insertion stock. We found that Wdr59 promotes the ability of the GATOR1 component Nprl2-T7-GFP^{11} to co-IP RagA in ovaries from both fed and starved females (Fig. 4 *A* and *B*). Thus, in *wdr59*^{1} ovaries, which have increased TORC1 activity, there is a decreased association between the TORC1 activator RagA and its inhibitor GATOR1. Conversely, increased levels of RagA were co-IPed by Nprl2-T7-GFP^{11} in *wdr24*^{1} mutant ovaries relative to WT ovaries. This is consistent with Wdr24 inhibiting the association of the GATOR1 complex with RagA, thus allowing the RagA^{GTP} form of the GTPase to recruit TORC1 to lysosomes for activation. These data support the model that Wdr59 inhibits TORC1 activity by promoting, directly or indirectly, the association of the GATOR1 complex with its target the Rag GTPase.

One way that Wdr59 might promote the association of GATOR1 with RagA is by relieving the inhibition of GATOR2 on GATOR1. To test this model, we examined the association between GATOR1 and GATOR2 in WT, *wdr59*^{1} and *wdr24*^{1} mutant ovaries by performing a Mio-Nprl3 co-IP with Mio-FLAG-GFP^{11} knockin. We determined that in absence of Wdr24, notably less Nprl3 was co-IPed by Mio-FLAG-GFP^{11} (Fig. 4 *C* and *D*). This is consistent with a decreased ability of the GATOR2 complex to inhibit GATOR1, in *wdr59*^{1} mutants resulting in decreased activity of GATOR1 toward RagA and increased TORC1 activity. Conversely, in ovaries from *wdr59*^{1} mutants, Mio-FLAG-GFP^{11} had an increased ability to co-IP Nprl3 relative to ovaries from WT or *wdr24*^{1} mutant females (Fig. 4 *C* and *D*). Thus, in the absence of Wdr59, the association of GATOR1 with its inhibitor GATOR2 is increased. Unexpectedly, we found an increased association of Mio-FLAG-GFP^{11} with Nprl3 in starved versus fed conditions. The reason for this unexpected result is currently not clear. Taken together, our data are consistent with the model that Wdr59 attenuates the binding of GATOR2 to GATOR1 which increases the ability of GATOR1 to bind and inhibit the Rag GTPase complex resulting in increased TORC1 activity.

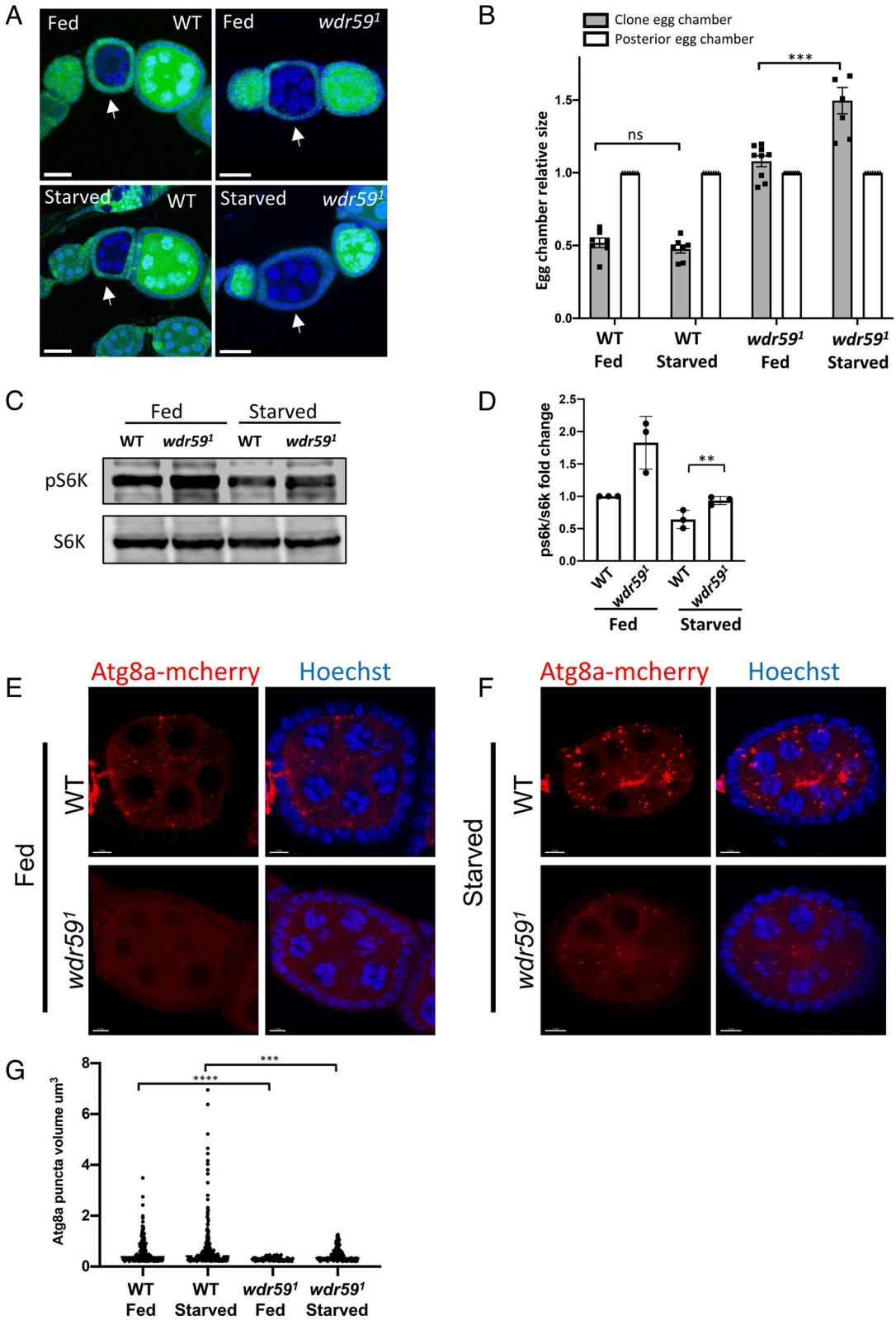

Fig. 2. *wdr59*[1] mutants have a reduced response to nutrient stress. (*A*) Ovaries from fed and starved females containing WT (control) and *wdr59*[1]mutant germline clones co-stained with Hoechst, to mark DNA (blue) and anti-GFP (green). The absence of GFP marks homozygous germline clones (white arrows). (*B*) Size quantification of *wdr59*[1]mutant versus WT germline clones performed as described in Fig. 1*F*. (*C*) Western blot of p-S6K and total-S6K levels of whole ovary lysates prepared from fed and starved (12 h) WT and *wdr59*[1]females. (*D*) Quantification of p-S6K levels relative to total S6K by Western blot (N = 3). (*E* and *F*) Egg chambers from (*E*) fed and (*F*) starved WT and *wdr59*[1]mutant females expressing Atg8a-3xmCherry (red), which marks autophagosomes and autolysosome, co-stained with Hoechst. (*G*) Quantification of Atg8a-mCherry puncta size (μm^3) in three independent stage 4 egg chambers. 5 μm Z-stack were used for measuring the volume of puncta by Imaris software from (*E* and *F*). (Scale bar, 20 μm.) (*A*), 5 μm (*E* and *F*). Unpaired Student's *t* test was used to calculate the statistical significance. Error bars represent SD. ns: not significant, $^{**}P < 0.01$, $^{***}P < 0.001$, $^{****}P < 0.0001$.

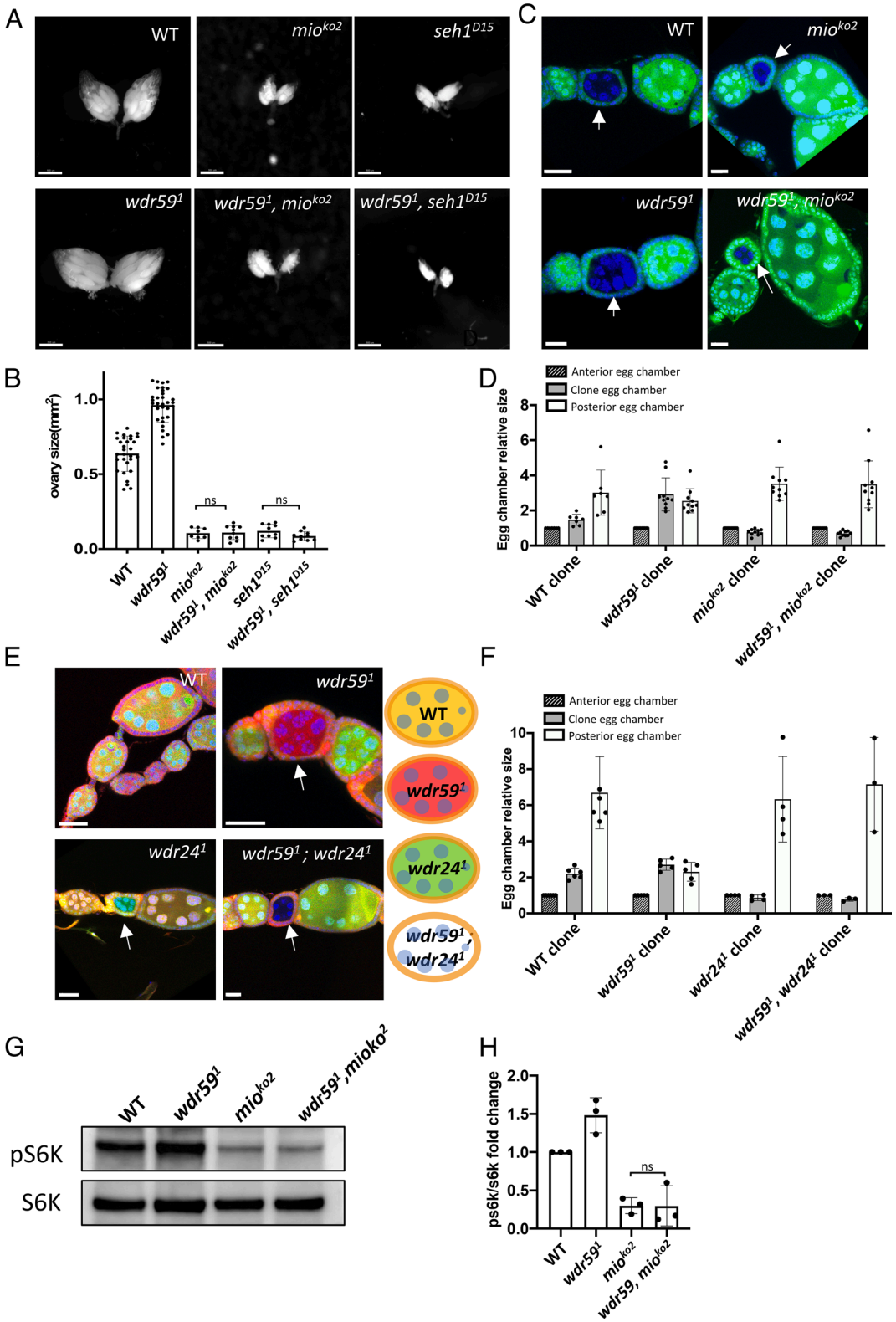

Fig. 3. The GATOR2 complex is epistatic to Wdr59. (*A*) Ovaries from Canton-S (WT), *wdr59*^{1}, *mio*^{ko2}*seh1*^{D15} single mutants, and *wdr59*^{1}, *mio*^{ko2}and *wdr59*^{1}, *seh1*^{D15} double mutants. (*B*) Quantification of ovary size (μm^2) from genotypes shown in (*A*). (*C*) Germline clones, marked by the absence of GFP (green) of WT, *wdr59*^{1}, *mio*^{ko2} single mutants and *wdr59*^{1}, *mio*^{ko2} double mutants. Note that double mutants of *wdr59*^{1}, *mio*^{ko2} phenocopy the *mio*^{k2}single mutants. (*D*) Relative size quantification of egg chambers containing *wdr59*^{1}mutant clones, calculated as described in Fig. 1*F*. (*E*) FRT40, *wdr59*^{1} and FRT82b, *wdr24*^{1}chromosomes were used to generate double-mutant germline clones marked by the absence of both GFP (green) and Red Fluorescent Protein (RFP) (red), respectively. Adjacent heterozygous *wdr59*^{1}/Ubi-GFP, *wdr24*^{1}/ Ubi-RFP egg chambers are yellow from both GFP and RFP expression, *wdr59*^{1} single clones are marked exclusively by RFP while *wdr24*^{1} clones are labeled exclusively by GFP. (*F*) Relative size quantification of egg chambers containing WT and mutant clones, calculated as described in Fig. 1*F*. (*G*) Western blot of p-S6K and total-S6K levels of whole ovaries from WT, *wdr59*^{1}, *mio*^{ko2} and double mutant of *wdr59*^{1} and *mio*^{ko2}. (*H*) Quantification of p-S6K levels relative to total S6K from (*G*) (N = 3). (Scale bar, 500 μm (*A*), 15 μm (*C*), and 20 μm (*E*).) Unpaired Student's *t* test was used to calculate the statistical significance. Error bars represent the SD. ns: not significant.

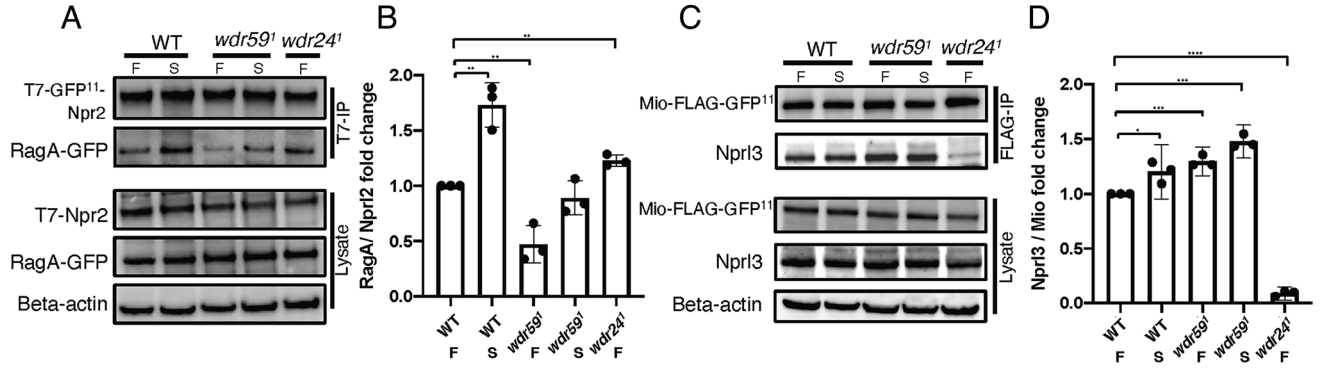

Fig. 4. Wdr59 promotes the association of GATOR1 with the Rag GTPase. (*A*) Ovaries were dissected from fed and starved, WT, *wdr59*^{1}and *wdr24*^{1} females carrying Nprl2-T7-GFP^{11} knockin and RagA-GFP genomic insertions. Ovarian lysates (input) from each genotype and condition were IPed with anti-T7 antibodies. Ovarian lysates and IPs were detected by Western blot using antibodies against T7, GFP, and Beta-actin. (*B*) Quantification of RagA levels relative to Nprl2 by Western blot from (*A*) (N = 3). (*C*) Ovaries were dissected from fed and starved WT, *wdr59*^{1}and *wdr24*^{1} females carrying the Mio-FLAG-GFP^{11} knockin and IPed with anti-FLAG antibody. Lysates (input) and IPs were detected by Western blot using GFP^{11}, Nprl3, and Beta-actin antibodies. (*D*) Quantification of Nprl3 levels relative to Mio by western blot from (*C*) (N = 3). Error bars represent SD. **P* < 0.05, ***P* < 0.01, ****P* < 0.001, *****P* < 0.0001. F: Fed, S: Starved.

Differential Requirements for Wdr59 and Wdr24 in the Localization of GATOR2 Components to Lysosomes. In *Drosophila*, components of GATOR1 (Nprl2, Nprl3, Iml1) and GATOR2 (Mio, Seh1, Wdr24) localize to lysosomes and autolysosomes (13, 14, 27). To determine the intracellular localization and of Wdr59, we generated a Wdr59-1xollas-3xGFP^{11} knockin transgenic fly. In live egg chambers, Wdr59-1xollas-3xGFP^{11} localized to Lamp1-3xmCherry puncta, a marker for lysosomes and autolysosomes, under both fed and starved conditions (*SI Appendix*, Fig. S4 *B–C*"). In response to nutrient stress, the Wdr59 puncta increase in size (*SI Appendix*, Fig. S4 *C–C*" and *E–E*"). We reasoned these larger puncta represented autolysosomes formed from the fusion of autophagosomes with lysosomes. Consistent with this idea, Wdr59-1xollas-3xGFP^{11} colocalized to Atg8a-3xmCherry puncta, a marker of autophagosomes and autolysosomes, in ovaries from both fed and starved females (*SI Appendix*, Fig. S4 *D–E*"). Next, we examined if the Wdr59 protein colocalizes with other GATOR complex components. We found that Wdr59-1xollas-3xGFP^{11} colocalizes with the GATOR1 component, Nprl3 and the GATOR2 component Wdr24 under both fed and starved conditions (*SI Appendix,* Fig. S4 *F–I'*). Thus, as is observed with other GATOR components, Wdr59 protein localizes to lysosomes and autolysosomes.

Next, we compared the role of Wdr59 and the GATOR2 component Wdr24 in the localization of the GATOR2 complex to lysosomes. Specifically, we examined the intracellular distribution of the knockin Mio-FLAG-GFP^{11} relative to the lysosomal/late endosome markers Lamp1 or Rab7 in *wdr59*^{1} and *wdr24*^{1}mutant egg chambers, respectively. In egg chambers from *wdr59*^{1} mutant females cultured under both fed and starved conditions, the tagged Mio protein colocalized to Lamp1 and Rab7 positive puncta (Fig. 5 *B* and *C* and *SI Appendix,* Fig. S5). Thus, Wdr59 function is not required for the lysosomal localization of Mio. In contrast, in egg chambers from fed females containing *wdr24*^{1} homozygous germline clones that were co-stained with the late endosome/lysosome marker Rab7, Wdr59-ollas-GFP^{11} and Mio-FLAG-GFP^{11} puncta were not present (Fig. 5 *D* and *E*). Western blot analysis demonstrated that protein levels of Mio and Wdr59 are not notably decreased in *wdr24*^{1} mutant ovaries (Fig. 5 *F–I*). These data indicate that Mio and Wdr59 are released into the cytosol, but not degraded, in the absence of Wdr24. Thus, Wdr24 but not Wdr59 is required for the lysosomal localization of the GATOR2 component Mio.

Wdr59 has a Tissue-Specific Impact on TORC1 Activity. Our results raised the following question, why does Wdr59 inhibit TORC1 activity in the *Drosophila* ovary, but promote TORC1 activity in cultured cells? We reasoned that the role of Wdr59 in TORC1 regulation might be context specific. To explore this possibility, we examined the requirement for Wdr59 in the regulation of TORC1 activity in two additional *Drosophila* tissues, the larval eye imaginal disc brain complex and the adult fat body. We found that, as is observed in the ovary, TORC1 activity is upregulated in the larval eye imaginal disc brain complex in *wdr59*^{1} mutants relative to wild type (Fig. 6*A*). In contrast, in the adult fat body, TORC1 activity of *wdr59*^{1} mutant is notably decreased (Fig. 6*B*). Why might mutations in *wdr59* have opposite effects on TORC1 activity depending on tissue type? One possible explanation is that the activity/stability of other GATOR2 components requires Wdr59 in some, but not all, cellular contexts. To test this hypothesis, we examined the levels of the GATOR2 protein Mio in different cell types that have high (ovary) versus low (adult fat body) TORC1 activity in *wdr59*^{1} mutants. We found similar levels of Mio protein in WT and *wdr59*^{1} mutant ovaries (Fig. 6*C*). Thus, Wdr59 is not required for the accumulation of Mio protein in these tissues. In contrast, in the adult fat body, the levels of the Mio protein were significantly lower in *wdr59*^{1} mutants relative to WT fat body (Fig. 6*D*). Taken together our data indicate that there is a tissue-specific requirement for Wdr59 in the accumulation of GATOR2 components in *Drosophila*.

RNAi knockdowns of *wdr59* result in low TORC1 activity in *Drosophila* S2 cultured cells and mammalian HEK 293 cells, similar to what is observed with RNAi knockdowns of the GATOR2 components *mio*, *seh1*, and *wdr24* (9). To better define the role of Wdr59 in TORC1 regulation, we examined a Wdr59 knockout HeLa line cell (Wdr59KO). We found that as is observed with knockdowns of other GATOR2 components in cultured cells, Wdr59KO HeLa cells have low TORC1 activity. Next, we performed western blots to determine if the requirement for Wdr59 in HeLa cells is due to its role in the accumulation of GATOR2 components. Notably, Western blot analysis revealed that the levels of Mio and Wdr24 proteins were dramatically reduced in Wdr59KO cells (Fig. 6*E*). This result raised two related questions: 1) Are the levels of GATOR2 components decreased in the Wdr59KO cells due to degradation via the proteosome. Second, might increasing GATOR2 protein levels in Wdr59 mutants rescue TORC1 activity? To answer these questions, we treated Wdr59KO cells with the proteasome inhibitor MG132. First, we noted a dramatic increase in Mios and Wdr24 protein levels in Wdr59KO cells in the presence of MG132 (Fig. 6*F*). Additionally, this increase in GATOR2 protein levels correlated with increased TORC1 activity. Thus,

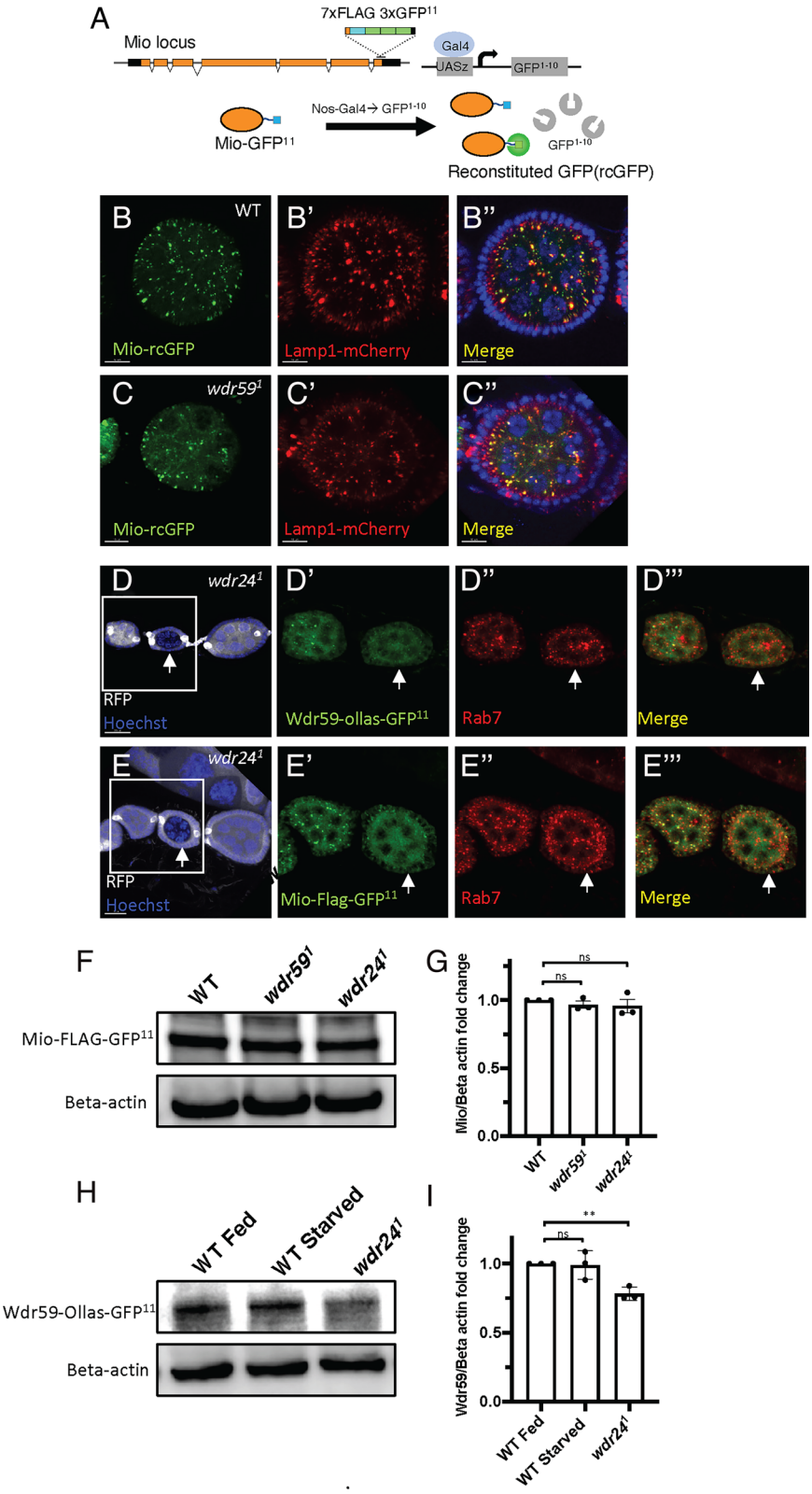

Fig. 5. Wdr59 is not required for the localization of GATOR2 components to lysosomes or autolysosomes. (*A*) Schematics illustrate the split-GFP tagging strategy to visualize endogenous Mio protein in the ovary. Three copies of split-GFP^{11} (3x GFP^{11}, green) and seven copies of FLAG epitope (cyan) were inserted into the end of the coding region of the Mio locus, immediately before the stop codon. Germline (NosGal4)-specific expressed split-GFP$^{1-10}$ (GFP$^{1-10}$) in the cytosol binds GFP^{11} on the C-terminus of Mio, constituting a functional GFP to indicate the location of the endogenous Mio protein. (*B–C″*) Live cell imagining of *Drosophila* egg chambers from females cultured on standard fly medium. Mio-rcGFP colocalizes with the lysosomal marker Lamp1-mCherry in (*B–B″*) WT and (*C–C″*) *wdr59*^{1} mutant egg chambers. In contrast, in *wdr24*^{1} mutant germline clones (*D–D″*) Wdr59-ollas-GFP^{11} (green) and (*E–E″*) Mio-FLAG- GFP^{11} (green) fail to colocalize with the lysosomal marker Rab7 (Red). *wdr24*^{1} germline clones are marked by the absence of RFP (white). (*F*) Western blot of Mio total protein levels from ovarian lysates prepared from WT, *wdr59*^{1}, and *wdr24*^{1} mutant females. (*H*) Western blot analysis of Wdr59 total proteins levels from ovarian lysates prepared from WT (fed), WT (starved), and *wdr24*^{1} (fed) mutant females. (*G* and *I*) Quantification of Wdr59 and Mio protein levels from (*F* and *H*) (N = 3). (Scale bar, 10 μm (*B–C″*), 20 μm (*D–D″*), and 15 μm (*E–E″*).) Unpaired Student's *t* test was used to calculate the statistical significance. Error bars represent the SD. ns: not significant. **P* < 0.05, ***P* < 0.01, ****P* < 0.001, *****P* < 0.0001.

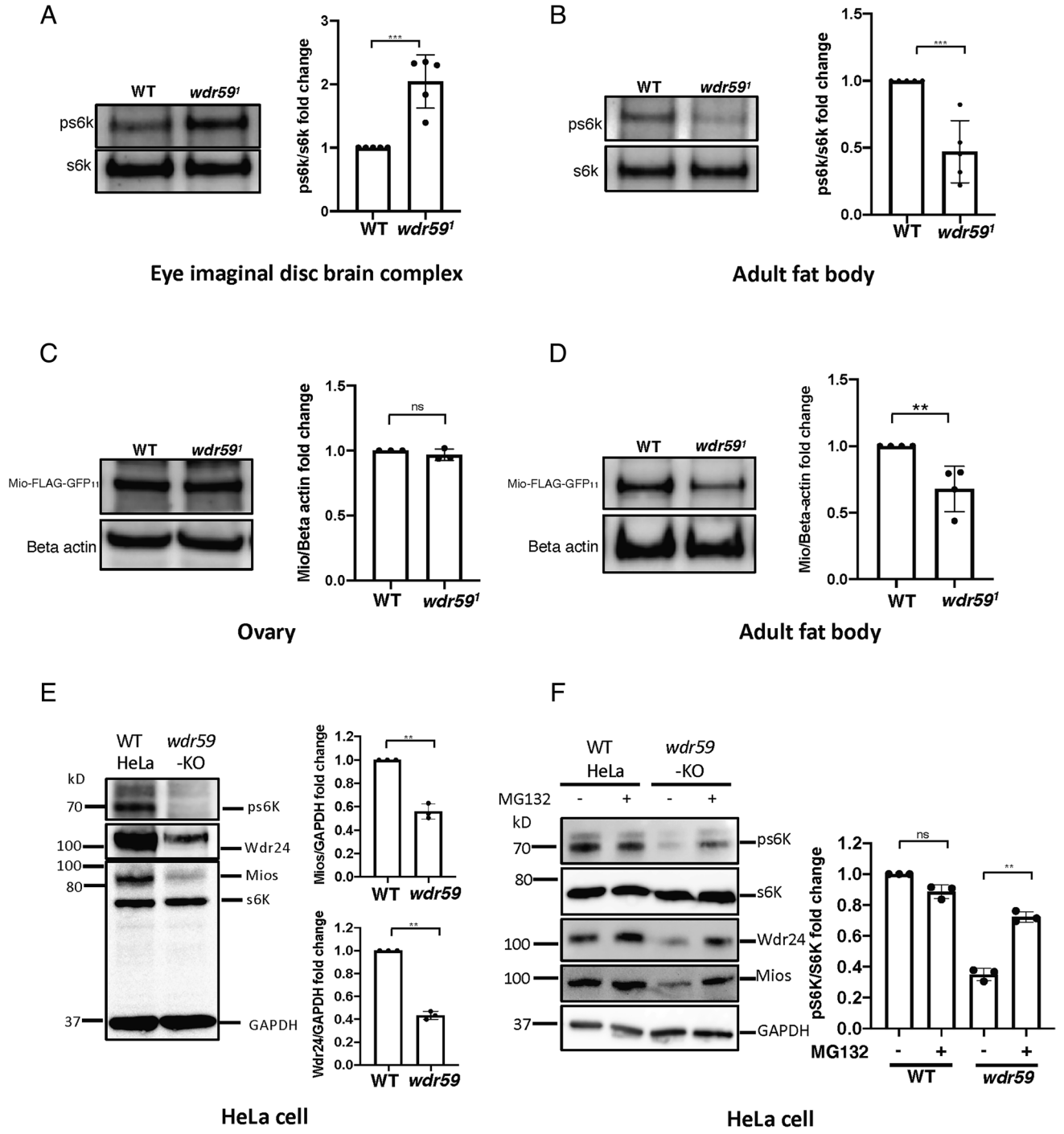

Fig. 6. Wdr59 promotes the accumulation of GATOR2 components in the adult fat body and mammalian HeLa cells. (*A* and *B*) Western blot of p-S6K and total-S6K levels in lysates prepared from larval eye imaginal disc brain complex and adult fat body dissected from WT and *wdr59*^{1} mutant animals. (*C* and *D*) Western blot of Mio total protein levels in ovary and adult fat body from WT and *wdr59*^{1} mutant females (*E*) p-S6K, S6K, Wdr24, and Mios protein levels in WT and *wdr59* mutant HeLa cells. (*F*) p-S6K, S6K, Wdr24, and Mios protein levels in WT and *wdr59* KO HeLa cells plus or minus the proteasomal inhibitor MG132. Note that addition of the proteasome inhibitor MG132 partially rescues both GATOR2 and p-S6K levels in Wdr59KO HeLa cells. Error bars represent the SD. ns: not significant. $^{**}P < 0.01$, $^{***}P < 0.001$.

these data are consistent with the hypothesis that decreased TORC1 activity observed in Wdr59KO cell line is due to this decrease in GATOR2 protein levels. Taken together, these data suggest that the role of Wdr59 in the accumulation of GATOR2 proteins may be conserved in *Drosophila* and mammals.

Discussion

The GATOR complex is an essential upstream regulator of TORC1 that is frequently mutated in human disease. Here we describe a dual function for the GATOR component Wdr59 in TORC1 regulation in *Drosophila*. Surprisingly, we find that Wdr59 functions to inhibit or promote TORC1 activity depending on cellular context. These studies broaden our understanding of the GATOR-TORC1 signaling axis in metazoans and demonstrate the importance of examining metabolic regulation in vivo.

In vivo studies often reveal tissue-specific and/or metabolic requirements for genes that are not observed in cell culture. In cultured cells from both mammals and *Drosophila*, RNAi depletions of *wdr59* result in decreased TORC1 activity and slow growth, thus

phenocopying depletions/knockouts of the GATOR2 components *wdr24*, *seh1*, and *mio* (9, 13, 14). Based on these initial studies, Wdr59 was assigned to the GATOR2 complex, which promotes TORC1 activity by downregulating the TORC1 inhibitor GATOR1. However, our in vivo studies indicate Wdr59 is not obligate member of the GATOR2 complex. Using *Drosophila* as a model, we find that *wdr59* mutant ovaries have increased TORC1 activity and growth rates and an attenuated response to nutrient stress. Notably, these phenotypes are the opposite of those reported for mutants of the GATOR2 components *mio*, *seh1*, and *wdr24,* but phenocopy those observed in mutants of the GATOR1 components *nprl2*, *nprl3*, and *iml1* (13, 30). Thus, in the *Drosophila* ovary, Wdr59 functions to restrict TORC1 activity. In line with these findings, we demonstrate that the binding of $RagA^{GTP}$ to the Nprl2 component of the GATOR1 complex is decreased in *wdr59* mutants, again the opposite of what we observe in mutants of the GATOR2 component *wdr24*. Taken together, these data suggest that Wdr59 inhibits TORC1 activity by increasing the activity of the TORC1 inhibitor GATOR1. Notably, recent evidence from *s. pombe* proposes that Wdr59, known as SEA3 in yeast, acts to inhibit TORC1 as a component of the GATOR1 complex (17). However, our epistasis analysis, as outlined below, indicated that in *Drosophila*, Wdr59 is not a component of the GATOR1 complex but instead functions as an inhibitor of GATOR2.

How might Wdr59 impact TORC1 activity? Biochemical, structural, and computational analysis from yeast indicate that SEA3/Wdr59 is well positioned to function as an interacting hub connecting GATOR2 with GATOR1 (32) Consistent with this observation, we find that, as is observed in fission yeast, Wdr59 regulates the interaction between components of the GATOR1 and GATOR2 complexes, with an increased association of GATOR2 with GATOR1 observed in the *wdr59* mutant background (17). Thus, one possible model to explain our data is that Wdr59 inhibits TORC1 activity by restricting the interaction of the GATOR2 complex with GATOR1, thus unleashing its GAP activity and TORC1 inhibitory potential. A prediction from this model is that components of the GATOR2 complex will be epistatic to Wdr59. In other words, Wdr59 requires the presence of an active GATOR2 complex to regulate TORC1 activity. Consistent with this prediction, we find that in the *Drosophila* ovary, *wdr59*, GATOR2 double mutants have a GATOR2-like phenotypes with reduced growth and TORC1 activity, strongly suggesting that GATOR2 is downstream of Wdr59 (Fig. 3). In contrast, in mutants or depletions of the GATOR1 components *nprl2*, *nprl3*, and *Iml1*, RagA remains in its TORC1-activating GTP-bound state, promoting the constitutive recruitment and activation of TORC1 on lysosomes independent of the status of GATOR2 (9, 12–14). Thus, GATOR1 components, unlike Wdr59, are epistatic to upstream members of the pathway including components of the GATOR2 complex (*SI Appendix,* Fig. S2) (9, 13, 14, 27). Taken together our data support the model that in *Drosophila*, Wdr59 is not required for GATOR1 function but instead acts upstream of the complex to regulate the activity of the GATOR1 inhibitor GATOR2. Importantly, our data demonstrate that the GATOR2 complex can inhibit GATOR1 independent of the Wdr59 subunit.

Currently, there are conflicting reports on the role of Wdr59/Sea3 in the regulation of TORC1 activity. In *Drosophila* and mammalian cultured cells, as well as in mouse breast cancer tumors, Wdr59 promotes TORC1 activity while in fission yeast Wdr59 inhibits TORC1 activity (9, 17–19). Our results provide a potential explanation for this contradiction. We find that in *Drosophila*, Wdr59 either promotes or inhibits TORC1 activity depending on cell type. In the female germline and the eye imaginal disc brain complex, Wdr59 inhibits TORC1 activity. However, in the adult fat body, Wdr59 promotes TORC1 activity. Importantly, in the adult fat body, but not the ovary, Wdr59 is required for the accumulation of the Mio protein. Thus, a possible reason that *wdr59* mutant fat bodies have reduced TORC1 activity is that they do not have a functional GATOR2 complex. This model is consistent with our finding that the GATOR2 complex is downstream of Wdr59.

To further explore why Wdr59 promotes TORC1 activation in some cellular contexts, we examined the levels of GATOR2 proteins in Wdr59KO HeLa cells. We wondered if the TORC1 promoting function for Wdr59 observed in cultured cells might reflect the requirement for Wdr59 protein to accumulate components of the GATOR2 complex. Indeed, we found dramatically lower levels of the GATOR2 components Mios and Wdr24 in Wdr59KO HeLa cells due to proteolytic destruction by the proteosome. Strikingly, inhibiting the proteasome pharmacologically resulted in increased levels of GATOR2 proteins which was accompanied by a partial rescue of TORC1 activity. These data strongly suggest that the low TORC1 activity observed in Wdr59KD or Wdr59KO HeLa cells is due at least in part to the concomitant decrease in GATOR2 protein levels.

Taken together, our data support the model that Wdr59 either promotes or inhibits TORC1 activity depending on cellular context (Fig. 7). The GATOR-TORC1 signaling pathway is frequently cited as a potential target of pharmaceutical intervention because of its role in cancer and epilepsy. Thus, it is essential to have a full mechanistic understanding of the in vivo function of the GATOR complex in the regulation of TORC1 signaling and growth in metazoans.

One day prior to submission of this manuscript, a detailed cryo-electron microscopy structure of the human GATOR2 complex was published by Valenstein, Rogala, Sabatini, and colleagues (33). They report that GATOR2 is a large 1.1 Mda complex that forms a cage-like structure, built on a continuous scaffold. As previously described, GATOR2 complex components contain numerous features common to membrane coating complexes which can form scaffolds that alter the curvature of membranes (34). Consistent with our studies, the authors report that the two copies of the Wdr59 subunit mediate the association of GATOR2 with GATOR1. However, as discussed above, we find that Wdr59 opposes the association of GATOR2 with GATOR1 in several *Drosophila* tissues, the opposite of what is reported here in HEK293T cells. Whole animal studies in *Drosophila* have determined that there are unique tissue-specific requirements for multiple individual GATOR2 subunits, including Mio, Seh1, Wdr24, and now Wdr59 (14–16). Going forward, it will be fascinating to determine how GATOR2 structure mediates tissue-specific GATOR2 functions in vivo.

Materials and Methods

***Drosophila* Strains and Genetics.** Details of the strains used in this study were listed in Key Resources table (*SI Appendix,* Table. S1). All *Drosophila* stocks were maintained at 25 °C on JAZZ-mix *Drosophila* food (Fisher Scientific). Experimental animals were collected at 3 to 5 d posteclosion and well fed with dry yeast. 1× PBS was used for starvation treatments for 12 h.

Generation of Transgenic Lines.

***wdr59*^{1}:** *wdr59*^{1} null allele mutant was generated by p-element excision (PWdr59G7958),

2845 bp were deleted in *wdr59* genomic region (2L, location: 11091633 to 11094477, FB2021_03). (35)

***mio*^{ko2}:**

CRISPR Design. The CRISPR target sites were designed via flyCRISPR Target Finder Tool on https://flycrispr.org/target-finder/

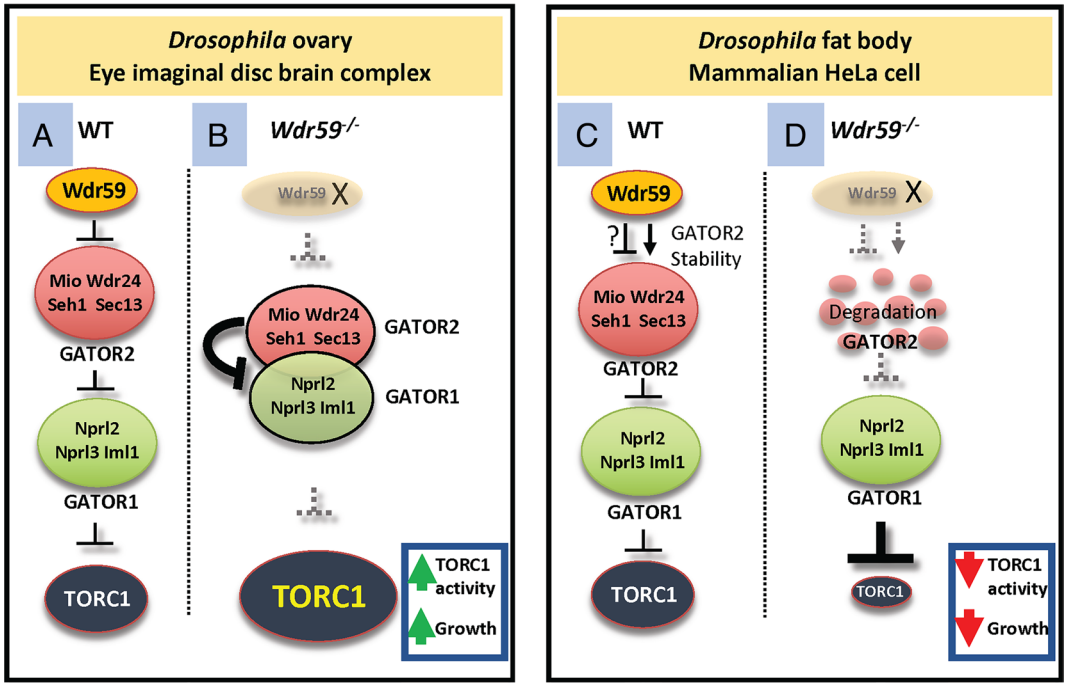

Fig. 7. A model for the dual role of Wdr59 in TORC1 regulation. (*A*) In WT animals, Wdr59 inhibits TORC1 activity upstream of the GATOR2 complex in the ovary and eye imaginal disc brain complex. (*B*) In *wdr59* mutants, GATOR2 increases its association with GATOR1, further inhibiting GATOR1 activity, and allowing for the increased activation of TORC1. (*C*) In the fat body of Drosophila and mammalian HeLa cells, Wdr59 protects GATOR2 components from degradation by the proteasome. (*D*) In the absence of Wdr59 in the Drosophila fat body or HeLa cells, GATOR2 components are destroyed by the proteasome, resulting in the derepression of GATOR1, an increased interaction of GATOR1 with RagA and a concomitant decrease in TORC1 activity. Please note the GATOR1 complex regulates TORC1 activity by acting as a GAP for the RagA component of the GTPase which functions to activate TORC1 (9). For clarity, RagA was left out of the above model.

Two Tandem gRNA was self-annealed and cloned into the BbsI site cut pCFD4-3xP3DsRed (Addgene 86864) via In-Fusion cloning (Takara). The construct was injected into attp40 to make a transgenic line.

Genomic Knockin. Genomic knockin was performed by CRISPR knockin as described previously with minor modification (36).

Western Blot Analysis. *Drosophila* ovaries were homogenized in RIPA buffer containing Complete Protease Inhibitors and Phosphatase Inhibitors (Roche). Antibodies were used at the following concentrations: rabbit anti-P-S6K T398 (1:1,000) (Cell Signaling), guinea pig anti-S6K (1:10,000) (PMID: 20444422), guinea pig anti-Nprl3 (1:1,000) (37), mouse anti-actin (1:10,000)(Abcam), rabbit anti-GFP[11] (1:1,000) (Bonopus), rat anti-OLLAS (1:1,000) (Novus), mouse anti-T7 (1:1,000) (Millipore sigma), and rabbit anti-GFP (1:1,000) (Cell signaling). The band intensity was quantified using Image J analysis tool (NIH).

Immunofluorescence and Live Imaging. Immunofluorescence was performed as previously described (15) using the following antibodies: rabbit anti-GFP[11] (1:1,000) (Bonopus), guinea pig anti-Nprl3 (1:1,000), and mouse anti-Rab7 (1:400) (Developmental Studies Hybridoma Bank). Anti-rabbit, anti-mouse, and anti-guinea pig Alexa Fluor secondary antibodies (Invitrogen) were used at 1:1,000. Nuclei were visualized by staining the DNA with Hoechst 33342 (Thermo Fisher, #H3570). Live-cell images were obtained as previously described (18).

Clonal Analysis. Ovaries were dissected in Schneider's medium from 2 d females after fed or starved treatment next used for staining or live imaging assays, genotypes are listed in *SI Appendix*, Table S1.

***Drosophila* Germ Cell Lysates Preparation and Co-IP.** Female flies were treated with regular fly food with yeast and/or starved 12 h, 30 pairs of ovaries were dissected on ice, lysed by RIPA buffer (Fig. 4*A*) or TLB buffer (Fig. 4*C*) (25 mM Tris-HCl pH 7.5, 5 mM magnesium chloride, and 0.5% Triton. 1× protease inhibitors) (38), containing Complete Protease Inhibitors (Roche), FLAG HA Tandem Affinity Purification Kit (Sigma) and Millipore T7 Tag Affinity Purification Kit were used for precipitation.

Atg8a Puncta Analysis. WT Atg8a-3xmCherry and *wdr59*[1]; Atg8a-3xmCherry female flies were treated with regular fly food with yeast or 12 h starved (1× PBS), ovaries were dissected in Schneider's medium then fixed with 4% PFA for 10 min, stained with Hoechst (1:10,000), imaged by confocal microscope, 5 μm Z-stack were used for measuring the volume of puncta, Atg8a-mCherry puncta size (μm^3) were auto-calculated by Imaris software, puncta <0.02 μm^3 are excised as background.

Cell Culture and Treatments. All mammalian cells were maintained and cultured at 37 °C, 5% CO_2, in high-glucose Dulbecco's modified Eagle's medium GlutaMAX-I with pyruvate, supplemented with 10% Fetal bovine serum (FBS) and 100 IU/mL Penicillin-Streptomycin (refer as the completed DMEM thereafter). WT HeLa cell was obtained from American Type Culture Collection (ATCC). Its identity was verified and tested for *mycoplasma*. Wdr59KO HeLa cell was made in the previous study (18).

Mammalian Protein Extraction and Immunoblot. HeLa cells were seeded into six-well plates. 1.2 million HeLa cells from each well were washed twice by PBS. Cells were then covered by 600 μL of the M-PER mammalian protein extraction buffer plus proteinases inhibitor cocktail with or without phosphatases inhibitor cocktail, followed by gently shaking at room temperature for 5 min. The solutions were collected, and the soluble parts were separated by centrifugation. Target proteins in the soluble part were detected by immunoblot using specific antibodies. To detect phosphorylated protein, Pierce Protein-Free T20 (TBS) Blocking Buffer was used to block the membrane and dilute the antibodies. HRP signals were visualized by using a ClarityTM Western ECL substrate kit (Biorad) and detected with a Biorad ChemiDocTM MP imaging system. The grey scale of each band was quantified by Photoshop CC. Each set of immunoblot experiments was repeated at least three times. Representative examples are shown in each figure.

Quantification and Statistical Analysis.
The details are shown in figure legends. All represent data from at least three independent experiments. Statistical comparisons were made using unpaired Student's *t* test provided by GraphPad Prism 8 software.

Data, Materials, and Software Availability. All study data are included in the article and/or at http://dx.doi.org/10.17632/rhzxf2fn89.1 *SI Appendix*

ACKNOWLEDGMENTS. Multiple stocks used in this study were obtained from the Bloomington *Drosophila* Stock Center supported by NIH grant P40OD018537. This research was supported by the Eunice Kennedy Shriver National Institute of Child Health and Human Development Intramural Research Program at the NIH (to M.A.L., HD00163 16).

Author affiliations: [a]Eunice Kennedy Shriver National Institute of Child Health and Human Development, National Institutes of Health, Bethesda, MD 20892

1. J. Simcox, D. W. Lamming, The central moTOR of metabolism. *Dev. Cell* **57**, 691–706 (2022).
2. A. Szwed, E. Kim, E. Jacinto, Regulation and metabolic functions of mTORC1 and mTORC2. *Physiol. Rev.* **101**, 1371–1426 (2021).
3. G. Y. Liu, D. M. Sabatini, mTOR at the nexus of nutrition, growth, ageing and disease. *Nat. Rev. Mol. Cell Biol.* **21**, 183–203 (2020).
4. A. Gonzalez, M. N. Hall, Nutrient sensing and TOR signaling in yeast and mammals. *EMBO J.* **36**, 397–408 (2017).
5. L. C. Kim, R. S. Cook, J. Chen, mTORC1 and mTORC2 in cancer and the tumor microenvironment. *Oncogene* **36**, 2191–2201 (2017).
6. E. Kim, P. Goraksha-Hicks, L. Li, T. P. Neufeld, K. L. Guan, Regulation of TORC1 by Rag GTPases in nutrient response. *Nat. Cell Biol.* **10**, 935–945 (2008).
7. Y. Sancak *et al.*, The Rag GTPases bind raptor and mediate amino acid signaling to mTORC1. *Science* **320**, 1496–1501 (2008).
8. Y. Sancak *et al.*, Ragulator-Rag complex targets mTORC1 to the lysosomal surface and is necessary for its activation by amino acids. *Cell* **141**, 290–303 (2010).
9. L. Bar-Peled *et al.*, A Tumor suppressor complex with GAP activity for the Rag GTPases that signal amino acid sufficiency to mTORC1. *Science* **340**, 1100–1106 (2013).
10. S. Dokudovskaya, M. P. Rout, A novel coatomer-related SEA complex dynamically associates with the vacuole in yeast and is implicated in the response to nitrogen starvation. *Autophagy* **7**, 1392–1393 (2011).
11. S. Dokudovskaya, M. P. Rout, SEA you later alli-GATOR - A dynamic regulator of the TORC1 stress response pathway. *J. Cell Sci.* **128**, 2219–2228 (2015), 10.1242/jcs.168922.
12. N. Panchaud, M. P. Peli-Gulli, C. De Virgilio, Amino acid deprivation inhibits TORC1 through a GTPase-activating protein complex for the Rag family GTPase Gtr1. *Sci. Signal.* **6**, ra42 (2013).
13. Y. Wei *et al.*, TORC1 regulators Iml1/GATOR1 and GATOR2 control meiotic entry and oocyte development in Drosophila. *Proc. Natl. Acad. Sci. U.S.A.* **111**, E5670–E5677 (2014).
14. W. Cai, Y. Wei, M. Jarnik, J. Reich, M. A. Lilly, The GATOR2 component Wdr24 regulates TORC1 activity and lysosome function. *PLoS Genet* **12**, e1006036 (2016).
15. T. Iida, M. A. Lilly, missing oocyte encodes a highly conserved nuclear protein required for the maintenance of the meiotic cycle and oocyte identity in Drosophila. *Development* **131**, 1029–1039 (2004).
16. S. Senger, J. Csokmay, T. Iida-Jones, P. Sengupta, M. A. Lilly, The nucleoporin Seh1 forms a complex with Mio and serves an essential tissue specific function in Drosophila oogenesis. *Development* **138**, 2133–2142 (2011).
17. T. Fukuda *et al.*, Tripartite suppression of fission yeast TORC1 signaling by the GATOR1-Sea3 complex, the TSC complex, and Gcn2 kinase. *Elife* **10**, e60969 (2021).
18. S. Yang *et al.*, The rag GTPase regulates the dynamic behavior of TSC downstream of both amino acid and growth factor restriction. *Dev. Cell* **55**, 272–288.e275 (2020).
19. M. Dai *et al.*, In vivo genome-wide CRISPR screen reveals breast cancer vulnerabilities and synergistic mTOR/Hippo targeted combination therapy. *Nat. Commun.* **12**, 3055 (2021).
20. M. Peng, N. Yin, M. O. Li, SZT2 dictates GATOR control of mTORC1 signalling. *Nature* **543**, 433–437 (2017).
21. Y. Wei *et al.*, The GATOR complex regulates an essential response to meiotic double-stranded breaks in Drosophila. *Elife* **8**, e42149 (2019).
22. K. Hahn *et al.*, PP2A regulatory subunit PP2A-B' counteracts S6K phosphorylation. *Cell Metab.* **11**, 438–444 (2010).
23. R. C. King, The meiotic behavior of the Drosophila oocyte. *Int. Rev. Cytol.* **28**, 125–168 (1970).
24. D. Drummond-Barbosa, A. C. Spradling, Stem cells and their progeny respond to nutritional changes during Drosophila oogenesis. *Dev. Biol.* **231**, 265–278 (2001).
25. L. LaFever, D. Drummond-Barbosa, Direct control of germline stem cell division and cyst growth by neural insulin in Drosophila. *Science* **309**, 1071–1073 (2005).
26. T. L. Pritchett, K. McCall, Role of the insulin/Tor signaling network in starvation-induced programmed cell death in Drosophila oogenesis. *Cell Death Differ.* **19**, 1069–1079 (2012).
27. Y. Wei, M. A. Lilly, The TORC1 inhibitors Nprl2 and Nprl3 mediate an adaptive response to amino-acid starvation in Drosophila. *Cell Death Differ.* **21**, 1460–1468 (2014).
28. C. Mauvezin, C. Ayala, C. R. Braden, J. Kim, T. P. Neufeld, Assays to monitor autophagy in Drosophila. *Methods* **68**, 134–139 (2014).
29. L. Bar-Peled, D. M. Sabatini, SnapShot: mTORC1 signaling at the lysosomal surface. *Cell* **151**, 1390–1390.e1391 (2012).
30. Y. Wei, B. Reveal, W. Cai, M. A. Lilly, The GATOR1 complex regulates metabolic homeostasis and the response to nutrient stress in Drosophila melanogaster. *G3 (Bethesda)* **6**, 3859–3867 (2016).
31. L. Bar-Peled, D. M. Sabatini, Regulation of mTORC1 by amino acids. *Trends Cell Biol.* **24**, 400–406 (2014).
32. R. Algret *et al.*, Molecular architecture and function of the SEA complex, a modulator of the TORC1 pathway. *Mol. Cell Proteomics* **13**, 2855–2870 (2014), 10.1074/mcp.M114.039388.
33. M. L. Valenstein *et al.*, Structure of the nutrient-sensing hub GATOR2. *Nature* **607**, 610–616 (2022), 10.1038/s41586-022-04939-z.
34. S. Dokudovskaya *et al.*, A conserved coatomer-related complex containing Sec13 and Seh1 dynamically associates with the vacuole in Saccharomyces cerevisiae. *Mol. Cell Proteomics* **10**, M110.006478 (2011).
35. H. J. Bellen *et al.*, The Drosophila gene disruption project: Progress using transposons with distinctive site specificities. *Genetics* **188**, 731–743 (2011).
36. J. Luo *et al.*, Antagonistic regulation by insulin-like peptide and activin ensures the elaboration of appropriate dendritic field sizes of amacrine neurons. *Elife* **9**, e50568 (2020).
37. Y. Zhou *et al.*, FKBP39 controls nutrient dependent Nprl3 expression and TORC1 activity in Drosophila. *Cell Death Dis.* **12**, 571 (2021).
38. K. Shen *et al.*, Architecture of the human GATOR1 and GATOR1-Rag GTPases complexes. *Nature* **556**, 64–69 (2018).